The Artificial Neural Network Structure Selection Algorithm in the Direct Task of Spectral Reflection Prediction

OLEG MILDER, DMITRY TARASOV, ANDREY TYAGUNOV
Department of IT and Automation
Ural Federal University
Mira 32 – R041, Ekaterinburg 620002
RUSSIA
datarasov@yandex.ru　　http://www.urfu.ru

Abstract: - Novel methods of digital image processing demand various approaches to spectral reflection prediction. The continuing complexity of the models leads to high requirements for computing power; however, this does not always contribute to the convenience and accuracy of forecasts. We offer an easy-to-use method for solving the direct problem of spectral reflection prediction using artificial neural networks. For color practitioners, prediction accuracy in terms of color difference is highly important. For researchers of artificial intelligence, the organization of the network learning process is of overriding interest. Those and other interoperates the necessary and sufficient minimum of the training sample to ensure satisfactory forecast accuracy. In this paper, we determine the size of such a sample. When training a network, we use spectral density instead of spectra. This provides a simplified simulation and improved accuracy of the forecast, which is confirmed experimentally.

Key-Words: - Spectrum, Color, Prediction, Artificial neural network, Image processing

1 Introduction

The goal of all color prediction models is to calibrate the color response of the color-reproducing (printing) system, based on the use of a standard set of colorants. In the print industry, when operating a substractive color model, the basic colors (the primaries) are cyan (C), magenta (M), yellow (Y), and black (K). The color response of the system is achieved using a superposition of these inks. Color prediction models account a given substrate, ink's type, given amounts of inks during the process of characterization and profile making and form the prediction of spectrum that might be measured when the test chart printed. Color prediction models may help the image processing software to decide, which set of inks and how to select and mix in order to create a determined color on a particular substrate by particular inks. The models need to account for both the interactions between inks and substrates and between light and the halftone print, as well as the Fresnel reflections and light scattering.

By the present time, a great deal of color prediction models have been developed.

Empirical surface models take into account only superpositions of ink halftones where reflected light is supposed to be a function of the effective ink surface coverage. These models do not account the light propagation within the print.

Physically inspired models engage a more detailed analysis of light-print interaction based on mathematical prediction of how light goes within a halftone print and what resulting color fade is.

Ink spreading models describe the physical dot gain as a difference between the effective and the nominal surface coverages. The models show how much an ink dot spreads out in all ink superposition conditions. They use the ink spreading curves mapping nominal surface coverages to effective surface coverages.

Spectral reflection prediction models are more complicated spectral color prediction models, which deal with spread-based and light propagation probability. They account the impact of different factors in print such as inks, substrate, the illumination conditions, the halftones influencing the range of printable colors and in creating printer characterization profiles for the purpose of color management [1]. One of the most applied one is the Kubelka–Munk model (1) that is widely used to predict the properties of multiple layers of ink overlaid at a given location, given information about each constituent ink's reflectance and opacity [2].

$$\frac{K(\lambda)}{S(\lambda)} = \frac{(1 - R_\infty(\lambda))^2}{2R_\infty(\lambda)}, \tag{1}$$

were K is absorption and S is scattering coefficients, R_∞ is the reflectance of an infinitely thick sample and the prediction of S and K from reflectance is made at a given wavelength λ. The formula (1) allows predicting the combined K and S coefficients for multiple inks:

$$K(\lambda) = K_B(\lambda) + \sum_{i=1}^{l} c_i K_i(\lambda), \qquad (2)$$

were B refers to the substrate, l is the number of ink layers, ci is the concentration and Ki is the absorption coefficient of the i-th layer. S(λ) is computed analogously.

Another widely applicable color prediction model is the Neugebauer model, which predicts the CIE XYZ tristimulus values of a color halftone patch as the sum of the tristimulus values of their individual colorants [3]. Since the Neugebauer model does not take into account the lateral propagation of light within the substrate (paper) and internal reflections at the paper-air interface it is often considered inaccurate.

Nowadays, the most promising model is the Yule–Nielsen modified spectral Neugebauer model (YNSN) where the Yule–Nielsen relationship applied to the spectral Neugebauer equations [4–7] (3).

$$R(\lambda) = \left(\sum_{i=1}^{p} w_i P_i(\lambda)^{\frac{1}{n}}\right)^n, \qquad (3)$$

were R(λ) is the reflectance of a halftone pattern neighborhood that is optically integrated as it is being viewed, wi is the relative area coverage of the i-th Neugebauer primary P, n is the Yule-Nielsen non-linearity that accounts for optical dot gain and is usually fitted by brute force.

Current CPMs accounting the physical dot gain are able to predict reflectance spectra as a function of ink surface coverage for up to 4 primaries [8]. The criterion for assessing the model's performance is minimization of the difference metric between measured and predicted reflection spectrum for each superposition condition. The most applicable difference metric used is CIE Lab dE (or ΔE) color difference [9–11]. The least dE formula that is being applied is the formula of 2000 year (dE2000).

In the work [12], we introduced 3D gradation trajectories as a further development of the common gradation curves. Implication the mathematical apparatus of differential geometry for gradation trajectories analysis in 3D CIE Lab space allows reveal their intrinsic features of curvature and torsion that help to improve ink limitation and color reproduction management in ink-jet. Further, we developed the idea of gradation trajectories and expand it to gradation surfaces [13, 14] that help to define a quasi-equal amount of inks to supply in order to obtain a precise color tone increment for two colorants.

All mentioned approaches have their advantages and drawbacks. Majority of models are too complicated to be embedded in a real-time digital image processing workflow without substantial development and adjustment that takes time. The empirical approach seems to be more promising; however, it also commonly requires a large number of printed tests for each pair of substrate-ink and ink overlays for assessments. Nevertheless, it is possible to find the minimal volume of the test chart to print that provides a satisfactory accuracy.

As a summary, one can note that quick and precise color prediction is still the issue that should be resolved. One of the promising way to build the quick-operating color prediction model is the artificial neural networks (ANNs) because this approach is suitable for solving complex nonlinear problems and has repeatedly proven its effectiveness, speed and undemanding to computing resources. This work is devoted to development of the ANN technique for color/spectral prediction. We offer an algorithm of network structure selection, build ANNs, predict of spectral reflection based on the recipes of initial colorants, and define the minimal volume of test charts to print with satisfactory predictive accuracy.

2 Experimental

For the experiment, we use the CMYK printer Konica-Minolta C6000L. Print mode: 1200×1200 dpi. Substrate: coated paper Murim NeoStar 120 g/m^2. The measurement tools: spectrophotometer x-Rite iOne iSis + x-Rite ProfileMaker package. Charts generation is made in ArgyllCMS package.

The approach we describe as follows: Print a specially developed test chart → Measure CIE Lab coordinates of the chart patches with a spectrophotometer → Build an artificial neural network using Matlab → Training the ANN until it reaches a particular condition (the training goal) → Predict spectral reflectance ρ(λ) by ANN using test chart patches recipes as ANN inputs → Assess the quality of prediction by the color difference formula dE2000 using a completely different validation chart as input. The main features of the algorithm are presented in Fig.1.

For the ANN development, we apply Matlab 16 package. The ANN type is a fully connected multilayer perceptron with one hidden layer. The number of hidden neurons vary from 6 to 15. The training techniques are Levenberg–Marquardt method with Bayesian regularization [15]. The trained network is stored in the form of a Matlab function. Further statistical operations are carried out in MS Excel and Statistica 10.
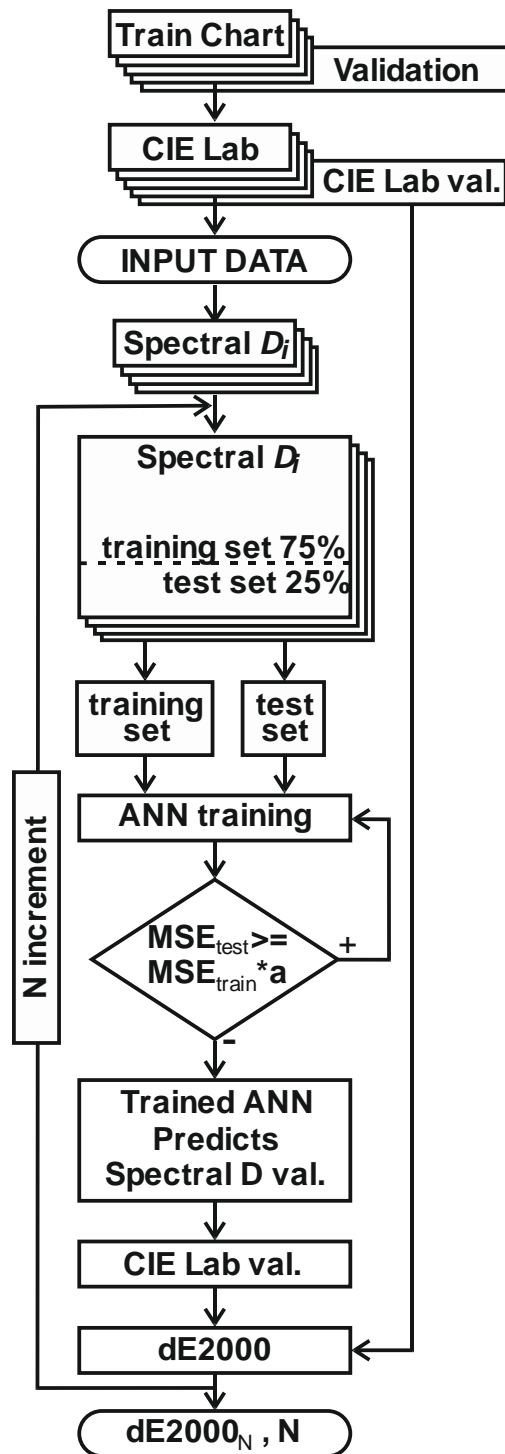
Fig. 1. The algorithm of the approach

For ANN prediction, the test chart is developed in ArgyllCMS. The ANN output is the predicted spectrum. For each spectra, CIE Lab coordinates are calculated. The test chart is then measured and the actual values of CIE Lab coordinates are established. The color difference between predicted and measured values for each patch of the test chart is calculated by dE2000 formula.

We predict the spectral reflectance (36 spectral zones from 380 to 730 nm, step 10 nm) by test chart patches recipes (4 values corresponding to CMYK percentage in the layout). Thus, the configuration of the network is $4 \times N \times 36 \times 36$, were N=6, 7, …, 15 is the number of neurons in the hidden layer. For the network training, we use four types of the training set, which is represented by so-called bodycube of different dimensions. It is the quasi-cube in the dimension of colors of the printing device. We apply the approach that is described in [16] (see also Fig.2) and extend it by application of the additional central recipe point. In terms of Fig. 2 it is (0.25, 0.25, 0.25, 0.25).
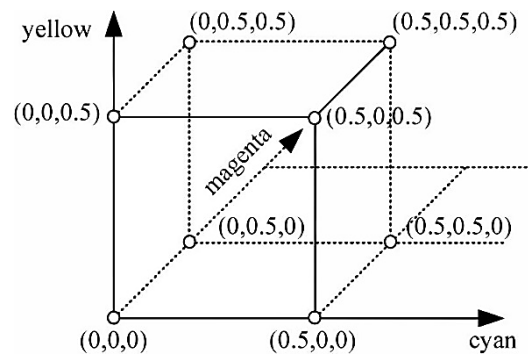
Fig. 2. Color cube in CMY color space

In the experiment, we use four different sets as bodycubes: bc3–bc6, were the digit indicates the number of gradations for each colorant. Thus, bc3 means that each of CMYK color recipes are obtained from a discrete sequence {0; 50; 100} for each color in all possible combinations. The central point is obtained from a discrete sequence {25; 75}.

In the training mode, the training set is randomly divided into training part (75%) and test part (25%). In order to avoid the overtraining, the training lasts until the residuals prediction errors (we use the mean squared error, MSE) in the test part surpasses training one in a times and above:

$$MSE.test \leq MSE.tr * a. .$$ (4)

For the training with relatively small amount of patches in the recipe, we apply several training cycles. In each cycle, division into training and test

parts is done every time again. The description of the training set composition is shown in Table 1. As may be seen from the Table 1, in the cases of short training sets (bc3, bc4), stop training conditions are softer than in volumetric sets (bc5, bc6).

TABLE 1. ANN TRAINING SET CONFIGURATIONS

Training set	bc6	bc5	bc4	bc3
Number of patches	1984	928	360	108
Stop training condition for 1 epoch, MSE.tr ≤	10^{-3}	10^{-3}	$3*10^{-3}$	$5*10^{-3}$
Stop training condition for all, a	1,1	1,1	1,15	1,3

The preliminary search has revealed that up to 7% of the predicted spectra have negative values in spectral components, which is physically impossible. This refers to cases where the actual value of the reflection coefficient is close to zero. ANNs, in the absence of restrictions, might chose negative values for predictions. However, currently, we do not have grounds for introducing restrictions. Moreover, they could complicate the model and may lead to higher computations requirements.

We solve the problem of negative values by the transition from the spectral reflection coefficients $\rho_i(\lambda)$ to the spectral optical density $D_i(\lambda)$ (4)

$$D_i(\lambda) = -\log_{10} \rho_i(\lambda), \forall\, i, \lambda ,$$ (4)

where i is the counter of patches, λ is wavelength, λ = {380, 390, …, 730}nm. While the reflection coefficient is inversely related to the amount of ink on the print, the optical density is directly proportional to the amount of dye applied or the percentage of filling the raster cell. Thus, the transition to optical densities can be considered as an attempt to embed a priori information into the network structure, which provides an increase in the accuracy of the prediction.

Thus, we train the ANN with spectral D and predict also values of spectral D. After the prediction, the spectral D values are recalculated back into the spectral reflectance (5). The predicting quality is assessed by color difference dE2000

$$\rho_i(\lambda) = 10^{-D_i(\lambda)}, \forall\, i, \lambda. \;.$$ (5)

The final stage of the experiment consists of application of the trained networks for spectral predictions. We feed (set as inputs) each of the trained networks with data of the independent validation set of recipes. This set contains 2790 patches randomly distributed over the color space of the printing device. This scale is built with a

particular limit: no less than a half of the patches must be located near the achromatic axis. Errors between factual and predicted spectra are evaluated by dE2000 formula. We also assess medians and 95% quantiles (Q95) of errors. The quantile is the upper bound of the color difference with 95% probability.

3 Results and Discussion

In the experiment, we create and train 40 different artificial neural networks (of the type of multilayer perceptron with one hidden layer). This value is formed by 4 training sets multiplied by 10 configurations. The number of training epochs in each training cycle are shown in Table 2. In each of 40 sets of errors we calculate medians and Q95 as assessments of mean and upper bound of prediction errors (see Table 3, Table 4, Fig.3, and Fig.4). The distribution that fit dE2000 best in most cases is lognormal. We use analytical distribution only for the ability to evaluate median and Q95.

TABLE 2. THE NUMBER OF TRAINING EPOCHS IN THE CYCLE

Number of neurons in the hidden layer	Number of training epochs in the cycle for the training set:			
	bc6	bc5	bc4	bc3
6	1	1	1	25
7	1	1	2	5
8	1	3	14	21
9	1	1	3	13
10	1	9	1	20
11	1	4	1	28
12	1	3	106	7
13	3	1	2	24
14	1	4	74	29
15	1	10	1	17
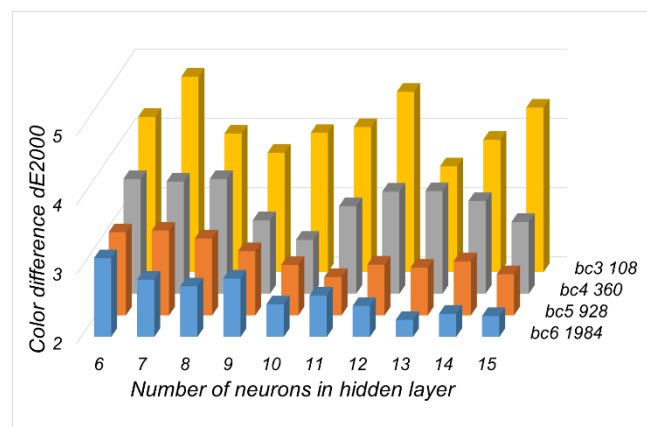
Fig. 3. Medians of dE2000 errors
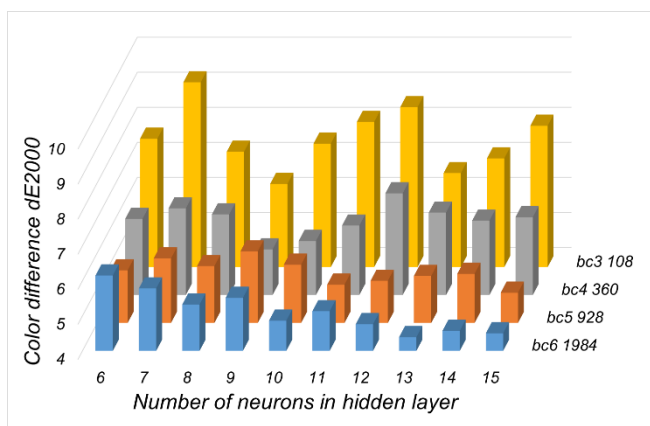
Fig. 4. Q95 of dE2000 errors

Figures demonstrate an obvious fact that more neurons and more patches in the training set lead to a better prediction results. However, there are clearly situations where the quality of the prediction obtained by a network trained on a small training set is quite satisfactory and comparable to the results obtained on large sets of input data.

In particular, a striking fact is observed for the bc4 set, where only 360 patches train 9 neurons and give a result comparable to the one for 13-14 neurons trained by more than 900 patches.

As Table 3 and Table 4 show, for the set bc6, the mean value of the color difference is just about 2,6 and 95% quantile is 5,1 that is quite good. At the same time, the smallest in volume bc3 with only 108 patches reaches the mean value of the color difference 4,13 and Q95=7,66 that also might be considered quite accurate.

TABLE 3. DE2000 MEDIANS

Training set:	bc6	bc5	bc4	bc3
Number of patches	1984	928	360	108
Number of neurons in the hidden layer	dE2000 medians			
6	3,14	3,20	3,66	4,24
7	2,83	3,23	3,62	4,82
8	2,73	3,11	3,66	4,00
9	2,84	2,93	3,06	3,72
10	2,47	2,73	2,78	4,01
11	2,60	2,55	3,27	4,09
12	2,45	2,73	3,47	4,60
13	2,25	2,69	3,48	3,53
14	2,33	2,78	3,34	3,91
15	2,30	2,59	3,04	4,38
Mean value	2,59	2,85	3,34	4,13

TABLE 4. DE2000 95% QUANTILES

Training set:	bc6	bc5	bc4	bc3
Number of patches	1984	928	360	108
Number of neurons in the hidden layer	dE2000 95% quantiles			
6	6,15	5,5	6,17	7,66
7	5,78	5,84	6,47	9,27
8	5,32	5,62	6,3	7,29
9	5,51	6,04	5,3	6,37
10	4,86	5,66	5,54	7,52
11	5,13	5,09	5,98	8,14
12	4,76	5,2	6,9	8,56
13	4,39	5,34	6,35	6,68
14	4,57	5,4	6,12	7,1
15	4,5	4,86	6,22	8,03
Mean value	5,10	5,46	6,14	7,66

In Fig. 5, the dependence of dE2000 medians on the number of patches in the training set scales for all number of neurons in the hidden layer is shown. The dotted line indicates the trend for the mean values.

We might suggest that this dependence should meet a power law (6)

$$dEmedian(x) = dEminimal + \frac{C}{x^n} \; , \qquad (6)$$

were x is a number of patches, C and n are some positive constants; in the model case, this dependence should not be less than some minimal value $dE_{minimal}$ and should asymptotically approach the ordinates axis.
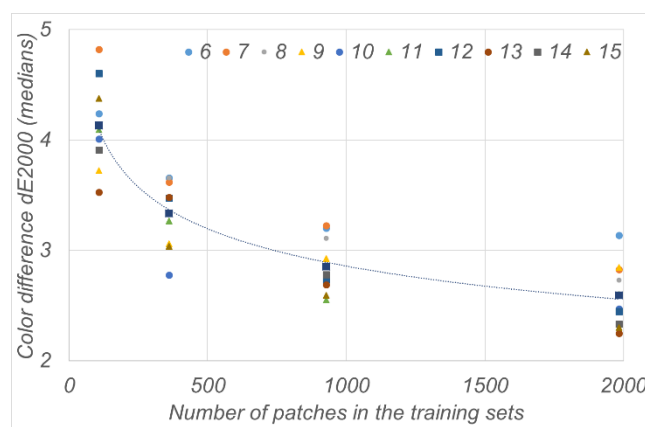
Fig. 5. Dependence of dE2000 medians on the number of patches in the training set for different number of neurons (6…15); dotted line is a trend

Moreover, the observed phenomenon of the presence of high prediction accuracy with the use of a smaller number of neurons can be explained by a

rather high dispersion of medians of color differences.

4 Conclusion

Artificial neural networks proved to be a convenient modeling tool, undemanding to computational resources and giving high accuracy of prediction. During the spectral reflection prediction by ANNs one may face with a problem of a framework construction. The approach might be the following: vary both, the volume of the training set and number of neurons in the hidden layer in order to obtain the target goals.

In our experiment, we show good prognosis abilities of the machine learning for all selected options. An unexpected result is the existence of combinations of ANN configurations and training conditions that give a satisfactory error of prediction with minimal computational demands (see the middle ranges in Fig. 3 and Fig. 4). This confirms the existence of a solution of the problem of the search of the minimum training set volume. Fig. 5 gives the possible range of such a solution: it lays between 100 and 500 patches.

The shape of the curve (6) is hyperbolic as it must have two asymptotes: minimal dE error and ∞ when the number of patches is zero.

References:
[1] Bala R. (2003) Device characterization. Digital Color Imaging Handbook, ed. G. Sharma (CRC Press, Boca Raton, FL), 269–379.
[2] Kubelka P. & Munk F. (1931) Ein Beitrag zur Optik der Farbanstriche, Zeitschrift für technische Physik, Germany, 12, 593–601.
[3] Neugebauer H.E.J. (1937) Die theoretischen Grundlagen des Mehrfarbendrucks. Zeinschrift fur Wissenschaftliche Photographie Photophysik Photochemie, 36, 36–73.
[4] Yule J. A. C. & Nielsen W. J. (1951) The penetration of light into paper and its effect on halftone reproductions. Proc. TAGA Conference 1951 (TAGA, Sewickley, PA), 65–76.
[5] Viggiano J. A. S (1990) Modeling the color of multi-colored halftones. Proc. TAGA Conference 1990 (TAGA, Sewickley, PA), 44–62.
[6] Hersch R.D. & Crété F. (2005) Improving the Yule–Nielsen modified spectral Neugebauer model by dot surface coverages depending on the ink superposition conditions. Proc. SPIE 5667, 434–445.
[7] Mazauric S., Hebert M., & Fournel T. (2018) Revisited Yule–Nielsen model without fitting of the n parameter. Journal of the Optical Society of America, 35, no.2, 244–255.
[8] Wyble D.R. & Berns R.S. (2000) A critical review of spectral models applied to binary color printing. Color Research & Application, 25, 4–19.
[9] Pauli H. (1976) Proposed extension of the CIE recommendation on "Uniform color spaces, color difference equations, and metric color terms". Journal of the Optical Society of America, Vol. 66, 866–867
[10] Hunt, R.W.G. (2004). The Reproduction of Colour, 6th rev. ed. Wiley & Sons, NJ. 724p.
[11] Hill B., Roger Th., Vorragen F.W. (1997) Comparative Analysis of the Quantization of Color Spaces on the Basis of the CIELAB Color-Difference Formula. ACM Transactions on Graphics, 16(2), 109–154.
[12] Milder O.B., Tarasov D.A., Titova M.Yu (2017) Inkjet Printers Linearization Using 3D Gradation Curves. CEUR Workshop Proceedings. Proceedings of the 1st International Workshop on Radio Electronics & Information Technologies (REIT 2017), Yekaterinburg, Russia, March 15, 2017. Vol.1814. 74–83.
[13] Milder O., Tarasov D. (2018) Ink-jet printer's characterization by 3D gradation trajectories on an equidistant color difference basis. Lecture Notes in Computer Science (LNCS). Vol. 10749. 40–52.
[14] Milder O., Tarasov D. (2018) Gradation surfaces as a method for multi-color ink-jet printers color specifications management. Lecture Notes in Computer Science (LNCS). Vol. 10749. 53–61.
[15] Kayri M. (2016) Predictive abilities of Bayesian regularization and levenberg-marquardt algorithms in artificial neural networks: A comparative empirical study on social data. Mathematical and Computational Applications. 21(2), 21020020
[16] Hersch R.D., Hebert M. (2015). Base models for color halftone reproduction. M. Kriss. Handbook of Digital Imaging, 2, Wiley, 1079–1132.